Available online at www.sciencedirect.com
ScienceDirect
International Journal of Thermal Sciences 47 (2008) 399–407
International Journal of Thermal Sciences
www.elsevier.com/locate/ijts

Dynamics and thermal behaviour of water sprays

A. Collin [a,*], P. Boulet [a], G. Parent [a], M.R. Vetrano [b], J.M. Buchlin [b]

[a] *Laboratoire d'Énergétique et de Mécanique Théorique et Appliquée (LEMTA), UMR CNRS 7563, Faculté des Sciences et Techniques, BP 239, 54506 Vandœuvre Cedex, France*

[b] *Von Karman Institute for Fluid Dynamics, Chaussée de Waterloo – 72, 1640 Rhode Saint Genèse, Belgium*

Received 20 February 2007; received in revised form 19 April 2007; accepted 30 April 2007

Available online 5 July 2007

Abstract

A detailed study (dynamics, thermal and radiative transfer) concerning a single water spray is presented. It is based on comparisons between experimental and numerical results. The experimental part of this work uses both the Global Rainbow Thermometry (GRT) technique, providing informations about the size distribution and the mean temperature of a set of droplets, and a Fourier Transform InfraRed (FTIR) spectrometer yielding the radiative attenuation through the spray. Besides a numerical simulation of the spray is done using an Eulerian–Lagrangian approach. The radiative transfer problem is treated by a Monte Carlo Method using a Ck model and the Mie theory in order to define the spectral radiative properties of the medium. Evaluation of the numerical reliability of the code regarding temperature level predictions and attenuation ability of the spray is allowed by the experimental results. Furthermore, the numerical simulation can explain some experimental observations: the Sauter mean diameter evolution inside the spray is for example clearly related to the polydisperse feature of the spray.
© 2007 Elsevier Masson SAS. All rights reserved.

Keywords: Single spray; Droplet; Radiative transfer; Simulation; Experiment; GRT

1. Introduction

The use of sprays is very important for a lot of engineering processes and industrial applications. In particular, water sprays are very useful for safety devices, like chemical protection against hazardous release of gases [1] or fire protection of people or goods [2–4]. This last example is the framework of our study. Here, the spray has to be used like a shield against radiation which comes from a fire. The spray, composed of water droplets and wet air, attenuates the radiation coming from a fire source.

The numerical simulation of the spray behavior is of major importance for the future industrial developments in order to understand the physical mechanisms which take place. The comparison of the numerical and experimental results has a double interest: to evaluate the reliability of a numerical code and to explain some physical phenomena inside the spray (the evolution of the droplet distribution as a function of the position in the spray, for example).

The study of a single water spray is carried out, associating results for the dynamics, heat transfer and in particular radiative transfer through the spray. The spray characterization concerning the droplet size distribution and the temperature has been performed at VKI (Von Karman Institute for Fluid Dynamics). Radiation transmission experimental evaluation and numerical results brought by simulations have been carried out at the LEMTA.

In a previous paper [5], the VKI has detailed and used the GRT in order to characterize a single flat fan spray. Informations have been obtained on the mean size variation, indicating in particular a Sauter diameter modification according to the vertical position in the spray. In addition, droplet temperature measurement feasibility thanks to the GRT was demonstrated. Experimental data have been registered and discussed in the case of an anisothermal spray (hot water in surrounding air).

In parallel, the LEMTA has recently undertaken the experimental study of the radiation attenuation through a similar spray [6]. Infrared transmissivity measurements have been car-

* Corresponding author. Tel./fax: (+33) 383 684 686.
E-mail address: anthony.collin@lemta.uhp-nancy.fr (A. Collin).

1290-0729/$ – see front matter © 2007 Elsevier Masson SAS. All rights reserved.
doi:10.1016/j.ijthermalsci.2007.04.010

Nomenclature

A_t	Attenuation	x, y, z	Cartesian coordinates
d_P	Droplet diameter ..... m	Y_f	Moisture ..... kg of water/kg of air
D_{10}	Arithmetic mean diameter ..... m	Δx	Cell size according to X-direction ..... m
D_{20}	Surface mean diameter ..... m	Δy	Cell size according to Y-direction ..... m
D_{30}	Volume mean diameter ..... m	ε	Dissipation rate of turbulent energy ..... $m^2\,s^{-3}$
D_{32}	Sauter mean diameter ..... m	ν	Wavenumber ..... cm^{-1}
f_v	Droplet volume fraction ... m^3 of water/m^3 of air	ρ_f	Density of the fluid phase ..... $kg\,m^{-3}$
$\mathcal{F}(z)$	Water quantity by length unit ..... m^3 of water/m of air	$\overline{d_{\ln}}$	Mean diameter for Log-Normal law ..... m
k	Turbulent kinetic energy ..... $m^2\,s^{-2}$	$\overline{\delta_{\ln}}$	Dispersion parameter for Log-Normal law
T_r	Transmissivity		
T_f	Fluid temperature ..... K		
U_f, V_f, W_f	Velocity of the fluid phase according to X, Y and Z-direction ..... $m\,s^{-1}$		

List of abbreviations

GRT	Global Rainbow Thermometry
MCM	Monte Carlo Method
FTIR	Fourier Transform InfraRed

ried out using a FTIR spectrometer. These experiments have been first simulated in a simplified 1D configuration and later in a companion study involving a 3D description of the spray combined with a specific postprocessing prediction of the radiative transfer [7].

The above mentioned experimental and numerical tools developed at the VKI and at the LEMTA are associated here in order to yield complementary information about the spray. The same laboratory nozzle device with the same pressure and flow rate conditions has been used by both groups. Results have been associated in order to allow comparisons and a complete analysis.

Experimental and numerical results for fluid dynamics and radiation attenuation by a water spray have been already presented in previous works [5–8]. Our study was based on a pioneer work by Dembélé et al. [9,10] and was extended to a tri-dimensional configuration, taking into account the coupling between spray flow and the radiative transfer. A first attempt was in particular reported in [7] for a similar spray regarding radiation attenuation. However, available data concerned few radiation transmission measurements, obtained for a weaker water flow rate. One originality of the present paper is that temperature and radiative data are presented and discussed in the same study. Details concerning the involved experimental setups will not be recalled here. A short description will be only given and attention will be paid to the discussion and the comparison of original results concerning temperature, size and radiation attenuation through the spray.

Through the association of their respective characterization methods, the two research groups have sought three goals:

- A test of a possible exploration of a spray in definite conditions using complementary techniques on two different laboratories;
- A comparison of the droplet temperature within the spray obtained by both numerical and experimental approaches allowing the validation of the numerical code regarding these data;
- An explanation through the numerical simulation for the mean Sauter diameter evolution.

In Sections 2.1 and 2.2, the GRT and the radiative measurement techniques are briefly presented. The numerical model is introduced in Section 3.1, involving an Eulerian–Lagrangian technique in order to simulate the spray. This technique gives a mean representation of the spray with average data (droplet volume fraction, diameter, temperature, ...). Section 3.2 deals with the particular problem of radiative transfer. Finally, results and comparisons between numerical and experimental data are presented in Section 4.

2. Experimental measurement techniques

In this section the experimental setups used in order to characterize the dynamics and the radiative behavior of a flat fan water spray are briefly described.

2.1. Droplet temperature and size measurements: GRT

The Global Rainbow Thermometry (GRT) [5,11–13] technique is a non-intrusive laser based technique that can provide the size and temperature probability distribution of an ensemble of droplets in a fixed probe volume. The experimental setup consists in an enlarged cylindrical laser beam of about 7 cm diameter that illuminates the droplets. The scattered light along the rainbow angle is forming a fringe pattern image recorded by a camera. A data inversion algorithm is used to obtain the temperature and the size probability distribution of the droplet from the absolute angular position of the fringes pattern in the space and from the fringes spacing. Tests reported in the result section correspond to the injection of hot water droplets (333 K) in surrounding air. The cooling of the dispersed phase can be followed as droplets are falling. This can be also simulated allowing comparisons between numerical data and experiments.

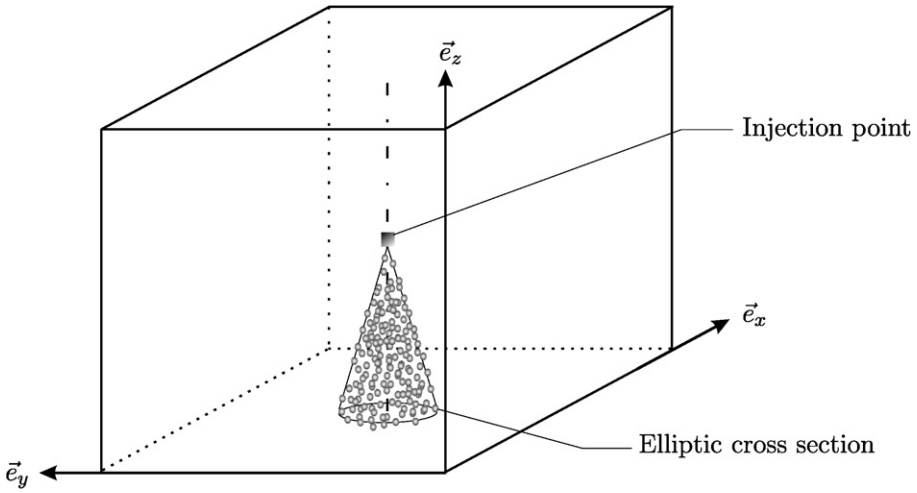

Fig. 1. Sketch of the injection in the room.

2.2. Experimental setup for the radiative measurements

A complete view of the experimental device has been detailed in a previous study [6]. A Fourier Transform Infra-Red (FTIR) spectrometer is used, in the spectral range 800–7500 cm^{-1}. Measurements are done with a 2 cm^{-1} spectral resolution. An incident radiation comes from the spectrometer within a small solid angle. This beam crosses the spray and is collected by a MCT detector. The measurements are done in the middle of the spray (centered according to Y-direction, see Fig. 1 for the spray orientation) for several heights 0.2, 0.4 and 0.6 meters below the injection point. The transmissivity is defined, thanks to the different signals obtained with and without the spray, by the ratio:

$$T_r = \frac{\text{outgoing flux with the spray on}}{\text{outgoing flux with the spray off}} \quad (1)$$

3. Numerical methods

Several models allow to describe the present two-phase flow. In the literature one fluid models [14], Eulerian–Eulerian models [15,16] and drop-size moments [17,18] are found with respective abilities and drawbacks regarding computational costs and closure model requirements. In the present study, an Eulerian–Lagrangian approach has been preferred. Using this approach, the particle trajectories can be finely described and interactions between phases are simply taken into account. Then, mean characteristics of the dispersed phase and spray geometry can be built in a preprocessing step. In particular, temperature of individual droplets or features of a given droplet class can be easily observed.

In order to generate the spray, a large number of droplets inside the spray have been followed. For each particle, position, velocity, temperature and size are tracked by integrating, step by step, the differential equation describing the motion of a single droplet [19]. The equation of motion is written by considering only the drag and gravity terms [7]. The evaporation model of Abramzon and Sirignano [20] with the assumption of infinite droplet conductivity is used. In the Lagrangian approach, each characteristic is instantaneous, whereas the Eulerian simulation only gives average data. A dispersion model is used, namely a first order stochastic model [21], in order to address the problem of the fluid turbulence influence on the particle motion during the Lagrangian steps. The representation of the spray is obtained by computing statistics for several averaged data (droplet volume fraction, temperature, velocity and mean size).

Due to the droplet fall, a turbulent air flow is generated. The motion of the gas phase is described by balance equations for mass, momentum and heat. In order to take into account the turbulence of the fluid and the droplet evaporation, a closure model for turbulence and a balance for moisture are considered in addition. The general standard 3D formulation of the balance equations is considered as described in [7], with source terms featuring the influence of droplets on the gas phase. A classical Finite Volume Method associated with a SIMPLE algorithm is used for the equation solution. The complete detail of the model can be found in Ref. [7], with a first validation case and a dedicated numerical sensitivity study.

The medium is characterized by radiative properties, namely the absorption coefficient, the scattering coefficient and the phase function [22]. Absorption effect is due to droplets and wet air, whereas the scattering phenomenon only comes from droplets. These radiative properties of the spray are computed using a Ck model [23] (for the gas phase) and the Mie theory [22] (for the droplets). The spectral discretization of these properties is imposed by the Ck model (using a Gaussian quadrature with 7 points), according to a 43-band model (for the spectrum between 1 to 60 μm). The radiative transfer problem is treated using a Monte Carlo technique [24,25]. This method has been chosen in order to best fulfill some properties of the medium, in particular the strong anisotropic scattering due to water droplets [26]. This numerical method uses an adaption of the so-called MCM 2 technique described in [27]. Quanta, which carry the radiative energy, are tracked through the medium, until their exit or the total absorption of their energies. In the medium, quanta travels following a straight line along a given distance of interaction. At the end of this path,

a new direction is sampled, in accordance with the scattering effect, using the phase function in a cumulative form. By this manner, the trajectories of quanta are built step by step. After the tracking of several quanta, a numerical post-processing allows to obtain the radiative fluxes exiting from the spray. Typically, after a sensitivity study reported in [7], 4×10^6 quanta are tracked in order to simulate the incoming spectral radiation, yielding more than 10^9 quanta for the computation of the total flux.

4. Comparison results

4.1. Experimental conditions and numerical details

The measurements are performed on a flat fan water spray, generated by a nozzle Spraying Systems TP 400067 with a flow number about 9.8×10^{-9} $m^3 s^{-1} Pa^{-0.5}$. The operating water pressure is set at 260 kPa, a value warrantied on both experimental setups through a pressure gauge and a regulation system. At the injection point, the temperature of the particles is about 333 K, whereas the temperature of the surrounding medium is 296 K and the relative humidity is 40%.

For the numerical simulation, the spray is injected in a closed room, with the following dimensions: 3 m × 3 m × 3 m sides. The used mesh is a non-uniform grid with 48 × 48 × 40 cells, specifically built for the present application and tested in order to verify that results are grid independent. The nozzle is located at a central position of this room and the spray is downward directed (see Fig. 1). The droplet distribution has been previously determined thanks to measurements at the VKI carried out 20 cm below the injection point. Numerically, a Log-Normal law with mean diameter and dispersion parameter equal to $\overline{d_{\ln}} = 110$ μm and $\overline{\delta_{\ln}} = 0.4$ respectively, has been used at the injection point. These parameters allow to match the droplet distribution with the experimental data 20 cm below the nozzle. Fig. 2 shows the probability density of the droplet volume fraction as a function of the size droplet classes. The Sauter mean diameter D_{32} (volume to surface mean diameter) is about 118 μm at the injection point. 20 classes are used in order to represent the polydisperse nature of the spray between 20 and 300 μm. Each class is related to 1/20 of the total flow rate (which is about 5×10^{-6} $m^3 s^{-1}$). The half ejection angles of the nozzle have been measured as 10° and 25° according to X-axis and Y-axis respectively (see Fig. 1).

Radiation outgoing from the FTIR device is a collimated beam with an angular divergence of 0.35°, in the X-direction. It is emitted by a globar at 1273 K. Detection is performed according to a solid angle equal to 8.7×10^{-6} sr.

4.2. Exploration regarding the droplet size evolution

Fig. 3 shows the Sauter mean diameter variation along the vertical axis of the spray. A reference case is presented and compared with other curves corresponding to a sensitivity study, performed varying a given parameter in each case. This will be commented later in the text. The reference case

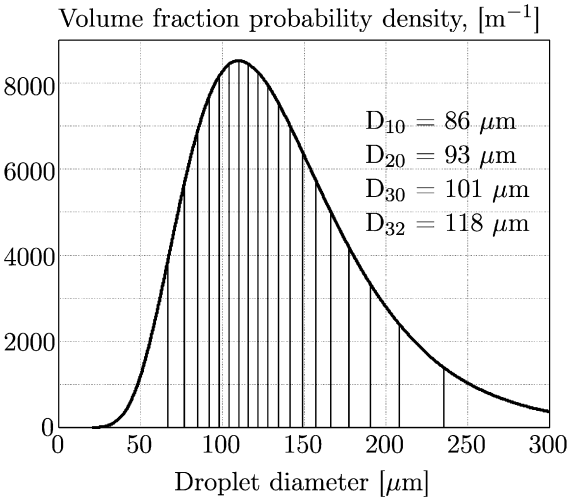

Fig. 2. Representation of the droplet volume fraction probability density according to the droplet diameter.

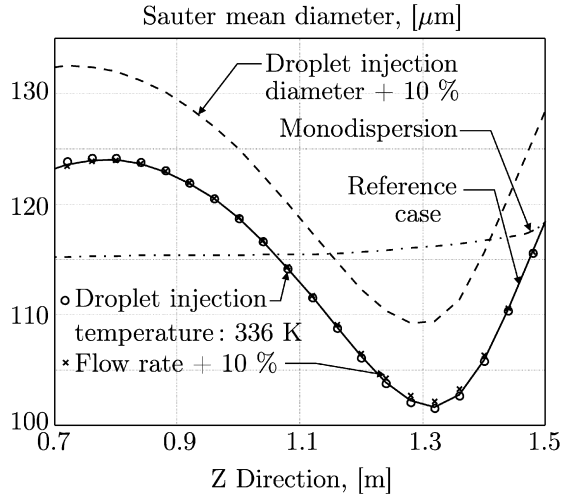

Fig. 3. Evolution of the mean Sauter diameter inside the spray as a function of vertical position.

representation is typically the one met in the experimental studies [5]. As can be seen, the Sauter mean diameter first decreases along 20 centimeters and then increases. Our previous studies have shown that the evaporation phenomena are not sufficiently effective to explain the first step of decrease [5,28] (in these laboratory experiments there is no extended strong heat source lighting the spray). Considering the low flow rate of the present laboratory nozzle (typically 0.005 L s^{-1}), the volume fraction is also so small that no collision effects are taken into account. Actually, the explanation comes from the polydisperse feature of the spray, as it will be seen.

The contributions of each droplet class may be separated with the numerical code. Fig. 4 gives five water quantity variations for five different droplet classes inside the spray with size centered around 60, 95, 125, 160 and 260 μm. The water quantity is defined as:

$$\mathcal{F}(z) = \sum_{x_i} \sum_{y_j} f_v(x_i, y_j, z) \Delta x_i \Delta y_j \tag{2}$$

where f_v is the droplet volume fraction at a given point with coordinates (x, y, z) inside the spray, Δx and Δy are the cell dimensions in the corresponding directions. $\mathcal{F}(z)$ is therefore an information about the water amount per meter as a function of the vertical position. This relation avoids the important variations of the droplet volume fraction according to the spray height, due to the use of a non-regular mesh. These curves provide an explanation for the evolution of the Sauter mean diameter, considering the following observations (see Fig. 4 for the water amount):

1. Below the injection point, droplets begin to decelerate (the initial velocity at the injection point is about 18 m s^{-1} whereas the fluid flow is around 4 m s^{-1}). This phenomenon particularly affects the velocity of the smallest droplet classes due to a weaker inertia. Then, their contribution to the volume fraction increases because the local number of small particles becomes higher than at the injection point. This results in a more important statistical weight in the calculation of the mean diameters. It explains why the Sauter mean diameter decreases few centimeters after the injection point.
2. Down in the spray, the influence of every droplet class deceleration is effective. The statistical weight of each class rises, with a shift from the injection point (see Fig. 4) as the diameter increases.
3. When the volume fraction of large particles becomes more important than the one of small droplets, the Sauter mean diameter increases.

Close to the ground (around $Z = 0$ m), the droplet volume fraction of the small particles (diameters about 60 or 95 μm) increases strongly. This corresponds to the air flow impacting against the bottom wall, where it is redirected laterally toward the outside of the spray and evacuated. The small droplets, which are mainly driven by the air flow, follow the fluid phase and consequently, the droplet volume fraction per meter ($\mathcal{F}(z)$) increases.

Figs. 5, 6 and 7 show spatial representations of sprays. Pictures have been obtained in a post processing step following and plotting the trajectory of some of the droplets in the converged spray (droplets randomly chosen for the illustration representing 0.01% of the total information left by all the droplets during the Lagrangian tracking). The polydisperse spray may be observed on Fig. 5. The shape of the spray illustrates the observations done experimentally with the present spray:

- a conic shape especially closed to the injection point,
- an elliptic cross-section,
- the influence of the turbulent dispersion, through the presence of several droplets outside the spray.

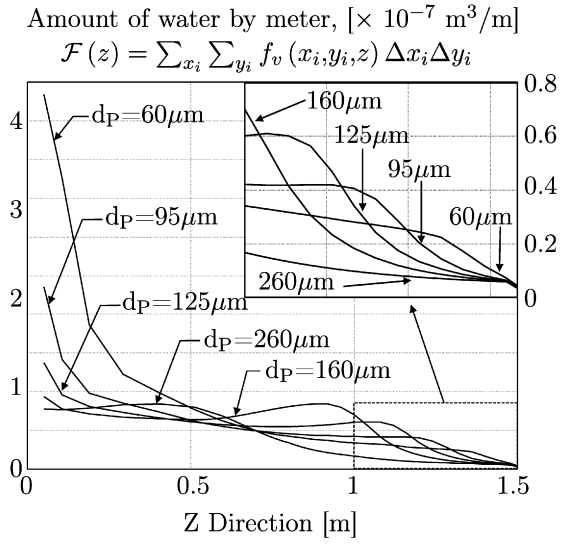

Fig. 4. Evolution of water amount inside the spray as a function of vertical position, contribution of five droplet classes.

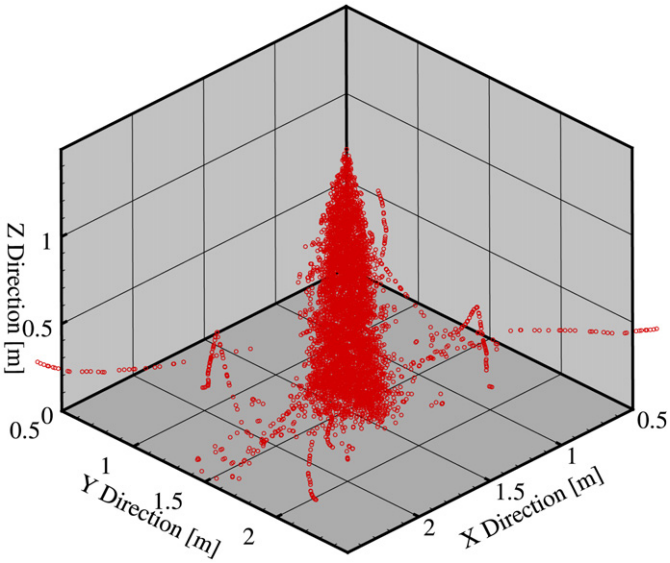

Fig. 5. Spray simulation through a selection of droplet trajectories.

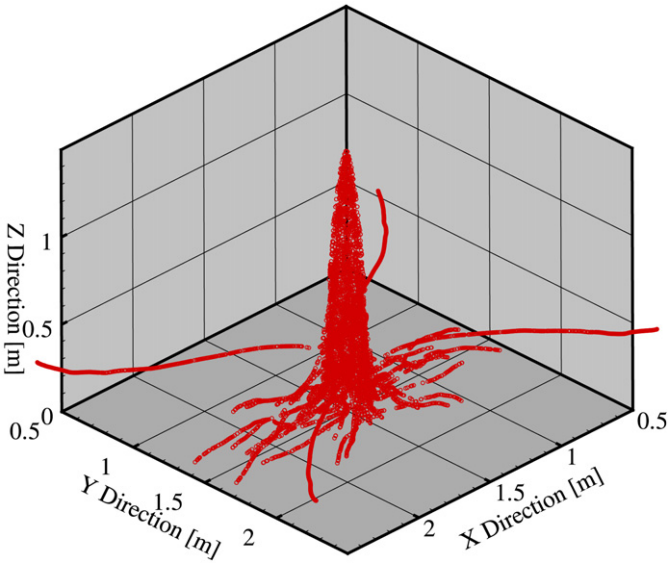

Fig. 6. Contribution of small droplets to the spray simulation.

Figs. 6 and 7 represent the spray pattern that two opposite droplet classes would produce (with diameter 60 and 260 μm respectively). The large droplet trajectories are not affected by the turbulent dispersion. Large droplets keep the direction given by their initial angles at the injection point during the first stage of their trajectory and then they fall vertically in a second step due to gravity influence. On the contrary, the small particle trajectories are quickly governed by the vertical air flow. These features are also observed experimentally where large droplets govern the shape of the spray, which is filled by small particles (especially located at the center of the spray).

The present numerical tool has been used in order to undertake some sensitivity analysis, in particular on the Sauter mean diameter. This may provide an information on the achievable numerical model accuracy or on the experimental uncertainty, depending on the studied point of view. Three parameters have been selected, being of huge importance for the simulation of the present experimental exploration: the mean diameter used in the Log-Normal law, the water flow rate and the droplet temperature at the injection point. In each case, new calculations have been considered in varying the parameter value by 10% for the mean diameter and the flow rate and modifying the injection droplet temperature: 336 K instead of 333 K. Only an increase in the input parameters is presented for the clarity of the illustrations. The results could be extrapolated and interpreted in the same manner with a negative variation of these values. In order to complete this sensitivity analysis, the same calculation have been done by substituting the polydispersion with a supposed equivalent monodispersion (keeping the same Sauter mean diameter at the injection). Results are presented on Fig. 3 in order to allow a comparison with the reference case. They show that, for the increase in the water flow rate or the droplet temperature, the Sauter mean diameter is exactly the same. These parameter evolutions are not important enough as to induce a different result, as a consequence of a modified spray hydrodynamics or an enhanced droplet evaporation. On the contrary, when varying the droplet injection diameter, the Sauter mean diameter is affected, increasing by 5% (which shows that the effect is non-linear). The results illustrate that this parameter is very important for the spray numerical simulation and must be carefully defined thanks to experimental means. For the present configuration, the results also show that the minimal value of the Sauter mean diameter is shifted to a location slightly farther from the injection point due to a simulated polydispersion with larger droplets. The monodispersion case exhibits a completely different evolution of the Sauter mean diameter, when compared with the reference case. The variation is weak, being solely due to the droplet evaporation. This phenomenon only results in a 3% evolution on the mean diameter, corresponding to an 8% change on the total water flow rate. If an accurate simulation of the mean diameter is sought, the approximation of a polydisperse spray to a monodispersion is not possible.

This set of numerical results is in accordance with the observations and the descriptions reported following the VKI measurements (see in particular [5]).

4.3. Droplet temperature analysis

Fig. 8 shows the mean temperature of droplets according to the Z-direction, comparing numerical and experimental data taken from Ref. [5]. The temperature profile is located at the center of the spray. The GRT measurements and the numerical predictions are in a good agreement and follow the same trend. Some thermocouple measurements are added for the comparison. Although some discrepancies can be observed, the results coming from the numerical simulation are perfectly in the range of measurement uncertainty. This error margin has two origins: the uncertainties on the measured values (as for all experiments) and the fact that GRT only takes into account near-perfectly spherical drops. In particular, this last point excludes some droplets with large size from measurements. The particles are cooled by convection with air flow and by evaporation. These combined effects explain the decrease of the temperature according to the Z-direction, when going down in the spray.

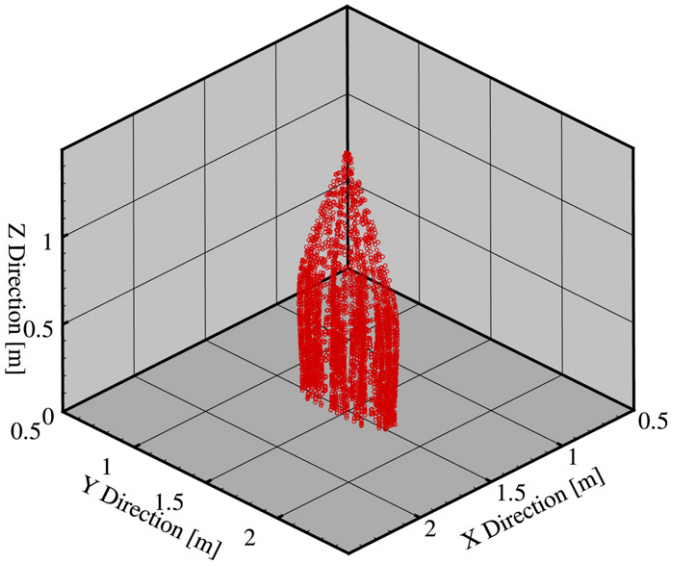

Fig. 7. Contribution of large droplets to the spray simulation.

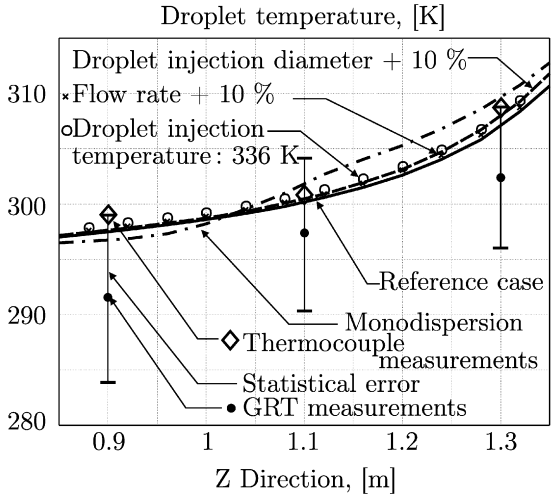

Fig. 8. Mean temperature of droplets as a function of vertical position ($Y = X = 1.5$ m). Experimental data taken from [5].

The numerical analysis presented on Fig. 8 shows a weak sensitivity of the droplet temperature to the tested parameters (as above-discussed, presented results only concern an increase in the input diameter, the flow rate and the initial droplet temperature). The simulation of a supposed equivalent monodispersion case yields results in a weaker agreement with the experimental case.

Fig. 9 shows the mean temperature of droplets according to the Y-direction. The axis used for this representation is at the center of the spray, 1.1 meters above the ground. In this second run of experimental acquisition, a weaker discrepancy between GRT and thermocouple measurements is observed. This second technique is rather a qualitative estimation of the temperature level. In any case data are close to those presented in the previous figure and the numerical estimations are in a good agreement with data provided by both measurement techniques. Between the middle and the edge of the spray, the temperature decreases. This evolution is in accordance with the fluid temperature which is larger at the center of the spray than at the edge, where temperature and moisture gradients induce an important heat transfer.

The sensitivity analysis shows the same trends as those presented on Fig. 8. This demonstrates that the droplet temperature is not very sensitive to the studied spray injection conditions.

The predicted evolution of the droplet temperature according to the Z-direction is plotted for five droplet size classes on Fig. 10. Initially, the temperature of each droplet is 333 K and the air flow is 296 K. The two reasons why small droplets are cooled more effectively than the largest particles are the followings. First of all, we have to consider that the smallest the particle size is, the longest the residence time is, thus allocating time for an actual change in the droplet temperature. Secondly, if surface and volume of the particles are both taken into consideration, the exchange area is larger for a collection of small particles, considering a given volume of water, than for large particles. These are two features enhancing the heat exchange between surrounding air and small droplets. During their fall, the droplets are first hotter than the fluid (see Fig. 10). During this stage, droplets are cooled by convection and evaporation phenomena. Droplet temperature would continue to decrease in the absence of convection with air, but when the temperature of particles becomes colder than the fluid one, a balance is reached between evaporation and convection. One can see that each droplet class converges to the same temperature (slightly lower than the fluid temperature as shown by Fig. 10).

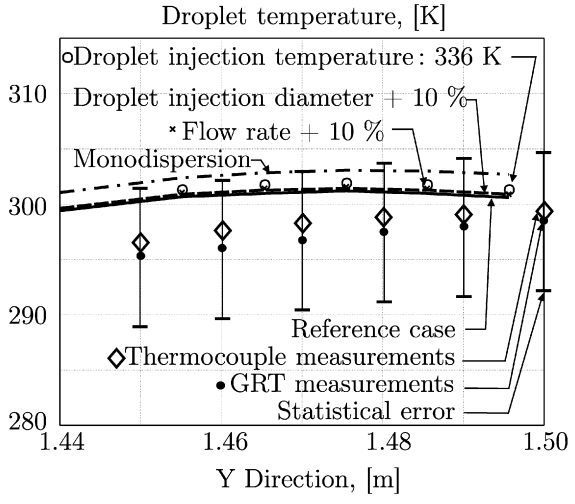

Fig. 9. Mean temperature of droplets in the transverse direction ($X = 1.5$ m, $Z = 1.1$ m). Experimental data taken from [5].

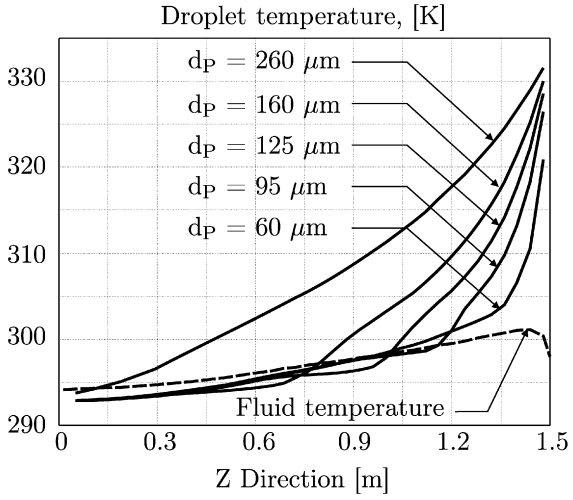

Fig. 10. Mean temperature of different droplet classes.

4.4. Radiative transfer through the spray

Our aim is to extend the experimental characterization and to compare the numerical estimations with the experimental measurements regarding radiation attenuation through the spray. The experimental setup and the measurement method are the same as previously described in [6]. Original experimental data have been taken for the present study at various vertical positions in the spray for the water pressure of 2.6 bars.

Fig. 11 presents such comparisons 20 centimeters below the injection point. We can observe that reference predictions (labeled "Numerical model") and measurements are in a good agreement. The discrepancy between the two curves can be

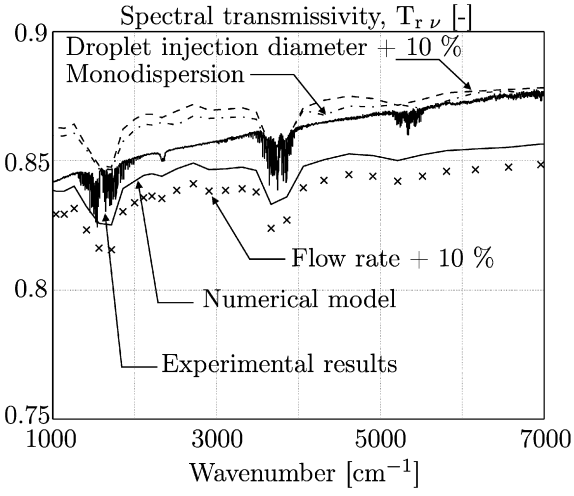

Fig. 11. Spectral transmissivity of the spray at 20 cm below the injection point.

explained considering an uncertainty on the transmissivity measurements, estimated around 1% [6], and an uncertainty on the droplet distribution introduced in the simulation.

The numerical results are in the confidence domain. The spectral dependence of the transmissivity is well reproduced. The transmissivity increases with the wavenumbers, with a slope governed by the scattering phenomena as observed in [6]. The influence of the gas phase is obvious through the presence of the three peaks located at 1600, 3760 and 5350 cm^{-1}. The contribution of water vapor is due to the increase of moisture inside the medium when the spray is on (due to droplet evaporation). This moisture rise is strong but the increase is not confined in the spray. This is taken into account in the numerical prediction since moisture is computed in the whole numerical domain and is used for the computation of the gas radiative properties. This influence is better simulated in the present attempt than in our previous test regarding radiation [7], thanks to a better knowledge of the experimental conditions. Data for the surrounding water moisture get from measurement have been introduced in the simulation. The present value of 40% for the surrounding air has led to an important rise of water vapor in the spray area with the spray on, leading to a noteworthy effect on the transmissivity curves for the vapor contributions.

As in the previous section, a sensitivity analysis has been carried out on the radiative transfer. The results on the same figure show that, for a 10% increase in the flow rate keeping the same droplet size distribution, the spectral transmissivity decreases by 1%. This effect is due to the amount of water which is more important than in the reference case, yielding a larger extinction ability. A symmetrical decrease in the flow rate (not shown here) would of course induce the inverse effect. The influence of the input droplet size has been also studied. The presented results concern a rise by 10% in the mean diameter at the injection and the case of a monodispersion (introducing the reference Sauter diameter as the input droplet size). For both cases the spectral transmissivity is seen to increase by around 2%. This can be explained by the increase in the droplet diameter, for the same water amount, which results in a reduction of the radiative properties (explained by the Mie theory) and consequently in a decreased attenuation.

Fig. 12 presents the same characteristics as Fig. 11 for different locations in the spray (40 and 60 cm below the injection point). Numerical predictions and experimental data are in a good agreement. The behavior of the transmissivity with respect to the vertical position in the spray is approximatively invariant. The results at 40 and 60 cm are very close, and the transmissivity is only little higher than the one obtained 20 cm below the nozzle. Once again, this behavior is well modeled with the numerical simulation, whereas it has been shown in [7] that this nearly invariant behavior of the transmissivity can not be observed, when the assumption of a monodipersion is used in order to simplify the simulation. This must be related to the lack of accuracy observed on the dynamics of the spray.

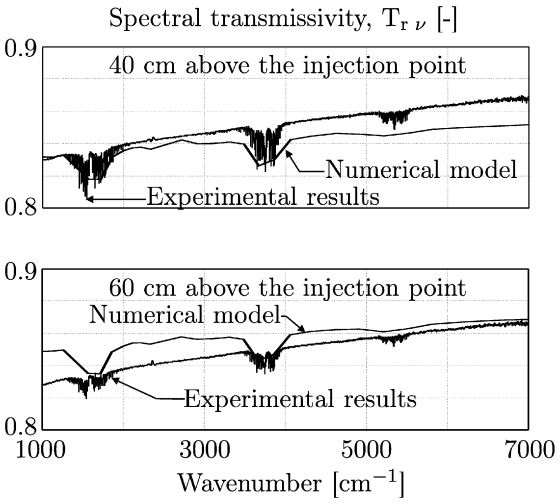

Fig. 12. Spectral transmissivity of the spray at 40 and 60 cm below the injection point.

5. Conclusion

Numerical and experimental data and corresponding comparisons have been presented for a single water spray. GRT and FTIR spectrometry techniques have been involved. A complete numerical simulation of the spray has been undertaken in parallel. The experiments allow to evaluate the reliability of the numerical code, whereas numerical simulations led us to explain some experimental observations. In particular, in this study, we have seen that the droplet deceleration in conjunction with their size is responsible for the Sauter mean diameter evolution inside the spray. Indeed, the polydisperse feature of the spray results in discrepancies in the influence of the droplets. Small ones first draw the mean size to a weaker value just below the injection point, whereas the largest ones induce an increase in the mean size when going far from the nozzle.

A second observation is that the droplet temperature obtained thanks to GRT experiments on a non-isothermal spray is reproduced by our simulation tool.

Finally a radiative transfer study has been conducted on the same spray, validating the efficiency of the numerical code on supplementary data. Attenuation has been observed to be nearly invariant with the vertical position in the spray along the first 60 cm on the present laboratory nozzle and in the present experimental conditions.

Here, the results predicted by the simulations are in good agreement with the experimental data at the present laboratory scale. A sensitivity analysis has shown a weak influence of the initial droplet temperature, whereas the input flow rate and the droplet diameter at the injection may have a stronger effect. Further tests are planned on more realistic conditions involved in fire protection, using a more important flow rate and a strong incident radiation. For the simulations, the following stage is to focus on industrial applications like safety devices against radiation emitted by flames. The aim will be to investigate some optimal configurations attenuating the total radiative flux through the spray with a minimized water consumption.

References

[1] J.M. Buchlin, Mitigation of problem clouds, J. Loss Prev. Process Ind. 7 (2) (1994) 167–174.

[2] J.L. Consalvi, B. Porterie, J.C. Loraud, Dynamics and radiative aspects of fire/water mist interactions, Combust Sci. Technol. 176 (5–6) (2004) 721–752.

[3] J.M. Buchlin, Thermal shielding by water sprays curtain, J. Loss Prev. Process Ind. 18 (4–6) (2005) 423–432.

[4] P. Boulet, A. Collin, G. Parent, Heat transfer through a water spray curtain under the effect of a strong radiative source, Fire Safety J. 41 (1) (2006) 15–30.

[5] M.R. Vetrano, S. Gauthier, J. Van Beeck, P. Boulet, J.M. Buchlin, Characterization of a non-isothermal water spray by global rainbow thermometry, Exp. Fluids 40 (1) (2006) 15–22.

[6] G. Parent, P. Boulet, S. Gauthier, J. Blaise, A. Collin, Experimental investigation of radiation transmission through a water spray, J. Quant. Spectrosc. Radiat. Transfer 97 (1) (2006) 126–141.

[7] A. Collin, P. Boulet, G. Parent, D. Lacroix, Numerical simulation of a water spray—radiation attenuation related to spray dynamics, Int. J. Thermal Sci. (2006), in press, doi:10.1016/j.ijthermalsci.2006.11.005.

[8] L. Zimmer, Étude numérique et expérimentale de la turbulence en écoulement gaz-gouttelettes. Applications aux rideaux d'eau en présence de vent latéral, PhD thesis, Université Henri Poincaré – Nancy I, France, 2001.

[9] S. Dembélé, A. Delmas, J.F. Sacadura, A method for modeling the mitigation of hazardous fire thermal radiation in water spray curtains, J. Heat Transfer 119 (4) (1997) 746–753.

[10] S. Dembélé, J.X. Wen, J.F. Sacadura, Experimental study of water sprays for the attenuation of fire thermal radiation, ASME J. Heat Transfer 123 (3) (2001) 534–543.

[11] J.P.A.J. Van Beeck, D. Giannoulis, L. Zimmer, M.L. Riethmuller, Global rainbow thermometry for droplet-temperature measurement, Opt. Lett. 24 (23) (1999) 1696–1698.

[12] J.P.A.J. Van Beeck, T. Grosges, M.G. De Giorgi, Global rainbow thermometry assessed by Airy and Lorenz–Mie theories and compared with phase Doppler anemometry, Appl. Opt. 42 (19) (2003) 4016–4022.

[13] M.R. Vetrano, J.P.A.J. Van Beeck, M.L. Riethmuller, Global rainbow thermometry: improvements in the data inversion algorithm and validation technique in liquid–liquid suspension, Appl. Opt. 43 (18) (2004) 3600–3607.

[14] E.E. Michaelides, Heat transfer in particulate flows, Int. J. Heat Mass Transfer 29 (2) (1986) 265–273.

[15] K. Prasad, C. Li, K. Kailasanath, Simulation of water mist suppression of small scale methanol liquid pool fires, Fire Safety J. 33 (3) (1999) 185–212.

[16] J.L. Consalvi, B. Porterie, J.C. Loraud, On the use of gray assumption for modeling thermal radiation through water sprays, Numer. Heat Transfer Part A 44 (5) (2003) 505–519.

[17] J.C. Beck, A.P. Watkins, On the development of spray submodels based on droplet size moments, J. Comput. Phys. 182 (2) (2002) 586–621.

[18] J.C. Beck, A.P. Watkins, On the development of a spray model based on drop-size moments, Proc. R. Soc. London, Ser. A 459 (2034) (2003) 1365–1394.

[19] M. Rüger, S. Hohmann, M. Sommerfeld, G. Kohnen, Euler/Lagrange calculations of turbulent sprays: the effect of droplet collisions and coalescence, Atomization Sprays 10 (1) (2000) 47–81.

[20] B. Abramzon, W.A. Sirignano, Droplet vaporization model for spray combustion calculations, Int. J. Heat Mass Transfer 32 (9) (1989) 1605–1618.

[21] S. Moissette, B. Oesterlé, P. Boulet, Temperature fluctuations of discrete particles in a homogeneous turbulent flow: a Lagrangian model, Int. J. Heat Fluid Flow 22 (3) (2001) 220–226.

[22] N. Berour, D. Lacroix, P. Boulet, G. Jeandel, Radiative and conductive heat transfer in a nongrey semitransparent medium. Application to fire protection curtains, J. Quant. Spectrosc. Radiat. Transfer 86 (1) (2004) 9–30.

[23] A. Soufiani, J. Taine, High temperature gas radiative property parameters of statistical narrow-band model for H_2O, CO_2 and CO, and correlated-k model for H_2O and CO_2, Int. J. Heat Mass Transfer 40 (4) (1997) 987–991.

[24] B.T. Wong, M.P. Mengüç, Comparison of Monte Carlo techniques to predict the propagation of a collimated beam in participating media, Numer. Heat Transfer Part B 42 (2) (2002) 119–140.

[25] R. Vaillon, B.T. Wong, M.P. Mengüç, Polarized radiative transfer in a particle-laden semi-transparent medium via a vector Monte Carlo method, J. Quant. Spectrosc. Radiat. Transfer 84 (4) (2004) 383–394.

[26] P. Boulet, A. Collin, J.L. Consalvi, On the finite volume method and the discrete ordinates method regarding radiative heat transfer in acute forward anisotropic scattering media, J. Quant. Spectrosc. Radiat. Transfer 104 (3) (2007) 460–473.

[27] P. Boulet, A. Collin, G. Parent, Monte Carlo simulation of radiation shielding by water curtains, in: Eurotherm 78—Computational Thermal Radiation in Participating Media II, Poitiers, France, 2006, pp. 53–62.

[28] A. Collin, Transferts de chaleur couplés rayonnement–conduction–convection. Application à des rideaux d'eau soumis à une intense source radiative, PhD thesis, Université Henri Poincaré – Nancy I, France, juillet 2006.